EUROPEAN ORGANIZATION FOR NUCLEAR RESEARCH

Proposal to the ISOLDE and Neutron Time-of-Flight Committee

Neutron capture cross section of ^{93}Zr

06/10/2011

G.Tagliente[1], P.M.Milazzo[2], M. Barbagallo[1], E.Berthoumieux[3], N.Colonna[1], *C.Guerrero[4], F.Käppeler[5], C. Lederer[6], C.Massimi[7], M. Mastromarco[1], A. Mengoni[8]*

[1] *INFN Sezione di Bari, Italy*

[2] *INFN Sezione di Trieste, Italy*

[3] *CEA-Saclay - Irfu, Gif-sur-Yvette, France*

[4] *CERN, Geneva, Switzerland*

[5] *Karlsruhe Institute of Technology, Institut fur Kernphysik, Karlsruhe, Germany*

[6] *Faculty of Physics, University of Vienna, Austria*

[7]Agenzia nazionale per le nuove tecnologie, l'energia e lo sviluppo economico sostenibile (ENEA), Bologna, Italy

[6] *Dipartimento di Fisica, Università di Bologna, and INFN Sezione di Bologna, Italy*

Spokesperson(s): G.Tagliente, P.M.Milazzo
(giuseppe.tagliente@ba.infn.it,paolo.milazzo@ts.infn.it)
Technical coordinator: [E.Berthoumieux,C.Guerrero] (eric.berthoumieux@cern.ch, carlos.guerrero@cern.ch)

CERN-INTC-2011-046 / INTC-P-310
06/10/2011

Abstract

We propose to measure the neutron capture cross section of the radioactive isotope ^{93}Zr. This project aims at the substantial improvement of existing results for applications in nuclear astrophysics and emerging nuclear technologies. In particular, the superior quality of the data that can be obtained at n_TOF will allow on one side a better characterization of s-process nucleosynthesis and on the other side a more accurate material balance in systems for transmutation of nuclear waste, given that this radioactive isotope is widely present in fission products.

Requested protons: 3x10^{18} protons on target, (split into 1 run over 1 year)

1. Introduction

The origin of the elemental abundances from iron to uranium can be almost completely assigned to neutron capture reactions by two main stellar scenarios, each being responsible for the production of about one half of the abundances in the mass region A≥56. Explosive nucleosynthesis related to supernovae or neutron star mergers is characterized by complex reaction networks involving short-lived and very neutron-rich nuclei. Because of the extremely high temperatures ($T>10^9$ K) and neutron densities ($n_n>10^{20}$ cm^{-3}) the time scale for neutron capture is of the order of milliseconds. Accordingly, this process is known as the rapid neutron capture process or r process [1].

The advanced burning phases of stellar evolution are periods of neutron capture nucleosynthesis by the slow s-process [1]. Depending on the stellar mass it operates in thermally pulsing low-mass Asymptotic Giant Branch (AGB) stars (main component) [2] or during core He and shell C burning in massive stars (weak component) [3].

Under s-process conditions temperatures are ≈ (1-9)×10^8 K and neutron densities can vary between ≈10^6 and 10^{11} cm^{-3}. Because typical neutron capture times are much larger than average half lives of β-unstable nuclei, the reaction path of the s-process follows the valley of stability by a sequence of neutron captures and β-decays once an unstable isotope is encountered.

Situated at and near magic neutron number N = 50, the zirconium isotopes take a particular position on the s-process path, just at the border between the weak and main component. Because of their magic or near magic neutron configurations all Zr isotopes exhibit relatively small (n, γ) cross sections. As far as the unstable isotope ^{93}Zr is concerned it can be considered as stable on the time scale of the s process because of its long half life of 1.5 Myr. This has the consequence that the daughter of ^{93}Zr, i.e., ^{93}Nb, is bypassed by the main s-process path. However, once the neutron flux is finished, ^{93}Zr is left to decay into ^{93}Nb (Fig. 1). The result is that the abundance of Nb follows that of Zr. It must be noted that ^{93}Nb is the only stable isotope of the element Nb.

Particularly interesting in this context are the presolar grains, which are microscopic, μm-sized stardust particles that have been recovered from primitive chondritic meteorites. Their isotopic compositions in a variety of major and trace elements, from C and O to Si, Mg, Sr, Zr, and Ba, differ by orders of magnitude from the composition of Solar System materials. These grains were shown to carry the signature of the nuclear reactions, which determined their production in individual parent stars. In fact, the Nb/Zr ratios observed in most grains are far from being satisfactorily explained with present ^{93}Zr cross section data [4].

Fig. 1 shows the s-process flow in the Zr-Mo region. No ^{96}Zr is produced if the neutron density is lower than about 5x10^8 cm^{-3}, and the s-process flux proceeds as illustrated by the solid yellow arrows. When the neutron density is as high as 10^{10} cm^{-3}, the ^{95}Zr branching point is open and up to 50% of the s-process flux goes through ^{96}Zr, producing an amount dependent on its cross section (orange arrow in Fig. 1). The neutron capture cross section of ^{93}Zr plays an important role in this reaction sequence as well as for explaining the ^{93}Nb abundance, which is produced by the subsequent decay of ^{93}Zr.

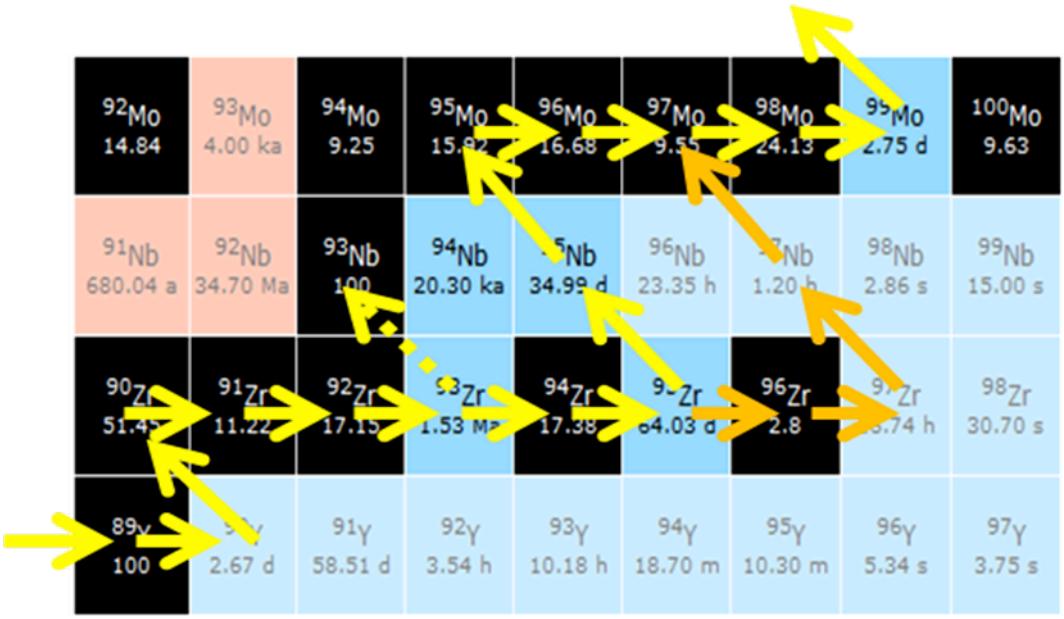

Figure 1: The s-process path around the Zr isotopes.

Apart from the impact on problems in Nuclear Astrophysics the neutron capture cross sections of the Zr isotopes are of interest of the advanced nuclear technology, because zirconium is widely used as constituent of cladding materials for fuel elements. ^{93}Zr, in particular, is one of the major long-lived fission products. Accordingly, the strong reduction of nuclear waste in advanced reactor systems and/or the transmutation of nuclear waste in dedicated systems already produced requests for high-accuracy data of the (n, γ) cross section of ^{93}Zr.

The Zr isotopes were included in the measurement campaign in the Phase 1 of n_TOF, in 2003 and 2004 [5-9]. The quality of obtained data in the study of these small neutron capture cross sections allowed for an important improvement of the accuracy and for resolving the discrepancies in previous data. As a consequence it has been possible to constrain the stellar conditions during the He burning stages of stellar evolution. In particular, this holds for the neutron magic nucleus ^{90}Zr, which accounts for more than 50% of natural zirconium and represents one of the key isotopes for the stellar *s*-process, because it acts as a bottleneck in the neutron capture chain between the Fe seed and the heavier isotopes [5]. Moreover, the neutron capture cross section of ^{91}Zr is also relevant to studies in nuclear structure, where the valence neutron of ^{91}Zr with respect to the neutron magic nucleus ^{90}Zr has interesting implications for the statistical analysis in the proximity of shell closures. Many resonances were observed for the first time in this isotope [6]. Concerning the study of the ^{92}Zr (n, γ) cross section the measurements performed at n_TOF provided a set of improved resonance parameters, thus reducing the cross-section uncertainties in the keV region to 5% as required for *s*-process nucleosynthesis studies and technological applications [7]. The (n, γ) cross section of ^{94}Zr has been measured with improved accuracy in the neutron energy range between 1 eV and 60 keV. At thermal energies of 8 and 23 keV, typical for the *s*-process in thermally pulsing low-mass AGB stars,

the MACS values were found to be slightly lower and 10% higher than reported in current compilations, respectively [8]. Further publications reporting the results obtained for ^{93}Zr and ^{96}Zr (n, γ) are in preparation.

2. The ^{93}Zr(n, γ) measurement performed at n_TOF (Phase 1) and existing data

In the measurement campaign during phase 1 of n_TOF also the unstable ^{93}Zr had been investigated. The characteristics of ^{93}Zr sample used in this measurement are listed in Table 1.

Table 1: Sample characteristics

Sample	Form	Isotopic composition (atomic %)						Thickness
		^{90}Zr	^{91}Zr	^{92}Zr	^{93}Zr	^{94}Zr	^{96}Zr	(atoms/b)
^{93}Zr	ZrO_2	2.29	18.61	18.95	19.98	20.50	19.67	0.00832

Because of its chemical form and its activity of 92.3 MBq, the sample had to be encapsulated in double canning: an internal 0.2 mm Al can, to contain the ZrO_2 powder, and an additional, external welded Ti can with 0.2 mm thick walls, to match the safety regulations for sealed radioactive samples.

Fig. 2 shows the measured capture yield of the sample (black) and the radioactive background (blue) using a pair of C_6D_6 liquid scintillation counters. The spectra are normalized to the acquisition time. The ^{93}Zr weighting function [10] and binding energy were used to extract the yield. It has to be noted that the high instantaneous flux of the n_TOF facility strongly reduces the background produced by the sample radioactivity.

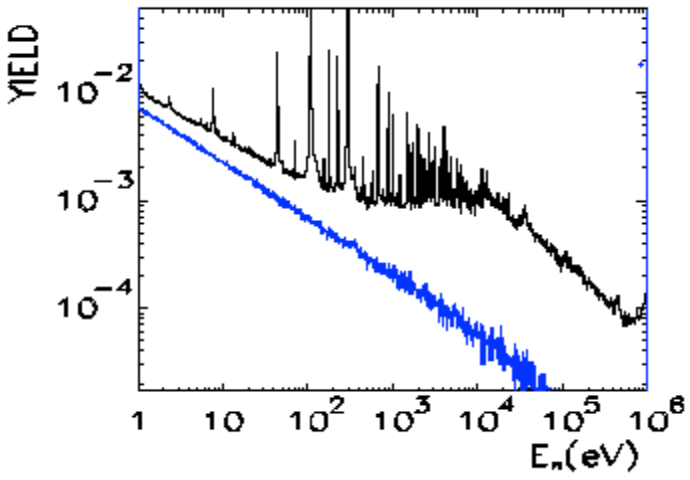

Figure 2. Capture yield of the sample used for the ^{93}Zr(n,γ) measurement (black) and background due to the activity of the sample.

In Fig. 3 the capture yield is shown (black after the background due to the sample activity had been subtracted. It illustrates that the overall background (red) is dominated by other sources of background, i.e. by neutron captures in the Ti can and by in-beam γ rays produced in the spallation target (concentrated in the energy range 1-100 keV).

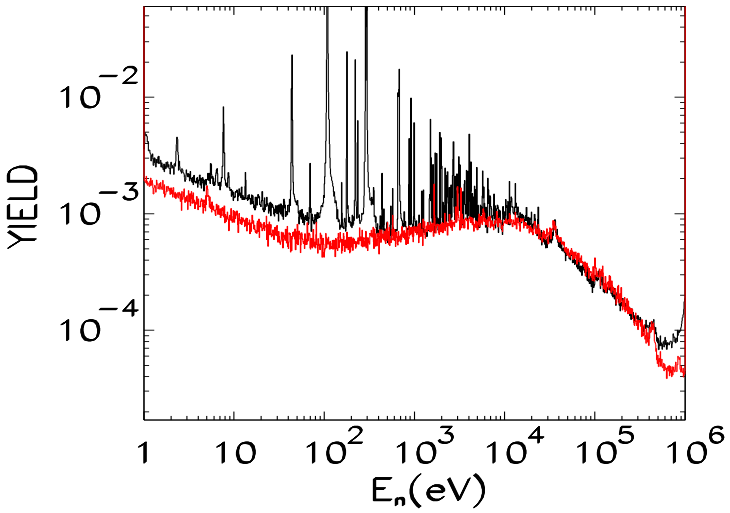

Figure 3: The ^{93}Zr(n,γ) capture yield (black) and the overall background (red).

Those backgrounds limited the neutron energy range that could be investigated to the region below 8 keV. The observed resonances were classified according to the composition of the sample, considering the isotopic impurities and the specific contaminations. Among the 63 resonances, which could be analyzed, four resonances were identified for the first time, whereas four of the resonances reported previously [11] have not been observed.

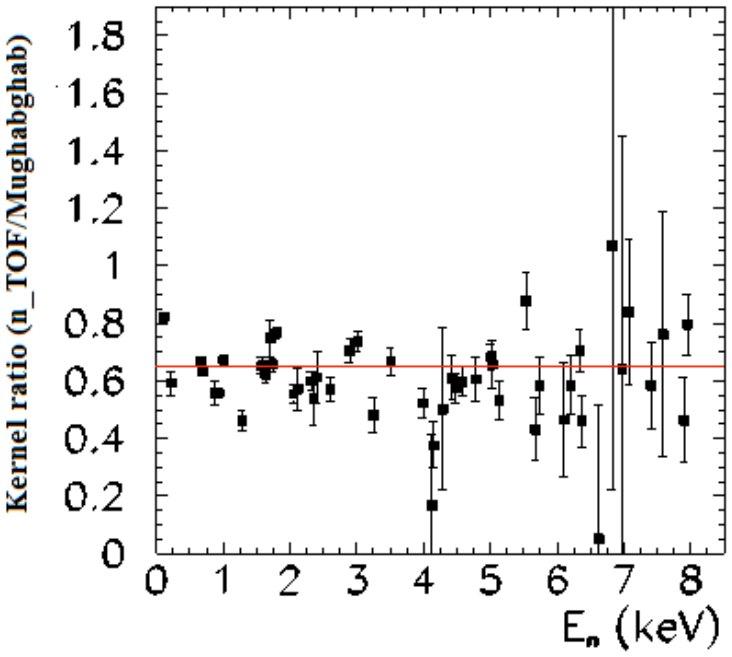

Figure 4: Ratio between ^{93}Zr capture kernel values extracted in the present measurement and the values reported in [11], versus resonance energy. The red line indicates the kernel ratio weighted average.

Fig. 4 shows the comparison between the capture kernels extracted in the n_TOF measurement and results reported in Ref. [11]. The capture kernel is related to the resonance parameters and is defined as $K = g\frac{\Gamma_n\Gamma_\gamma}{\Gamma}$, where Γ_n and Γ_γ are the neutron and radiative widths, respectively, $\Gamma = \Gamma_n + \Gamma_\gamma$ represents the total width, and g is the spin factor.

The significant difference of 35% that has been found on average, strongly affects the Maxwellian Averaged Cross Sections (MACS) for ^{93}Zr are shown in Fig.5. Note that the present data are limited to energies below 8 keV and had to be complemented with evaluated data [12], which dominate the calculated MACS for thermal energies above 10 keV. In view of the large discrepancy shown in Fig. 4, the MACSs were calculated for two extreme cases. In the first case, the evaluated data used to complement the measured resonances above 8 keV were not scaled, while in the second case they were scaled with a factor 0.65. Fig 5. shows the comparison of the present MACSs with the values from the compilation of Bao et al. [13]; data from the present work are shown as a band drawn inside the two extreme cases used to calculate the MACS.

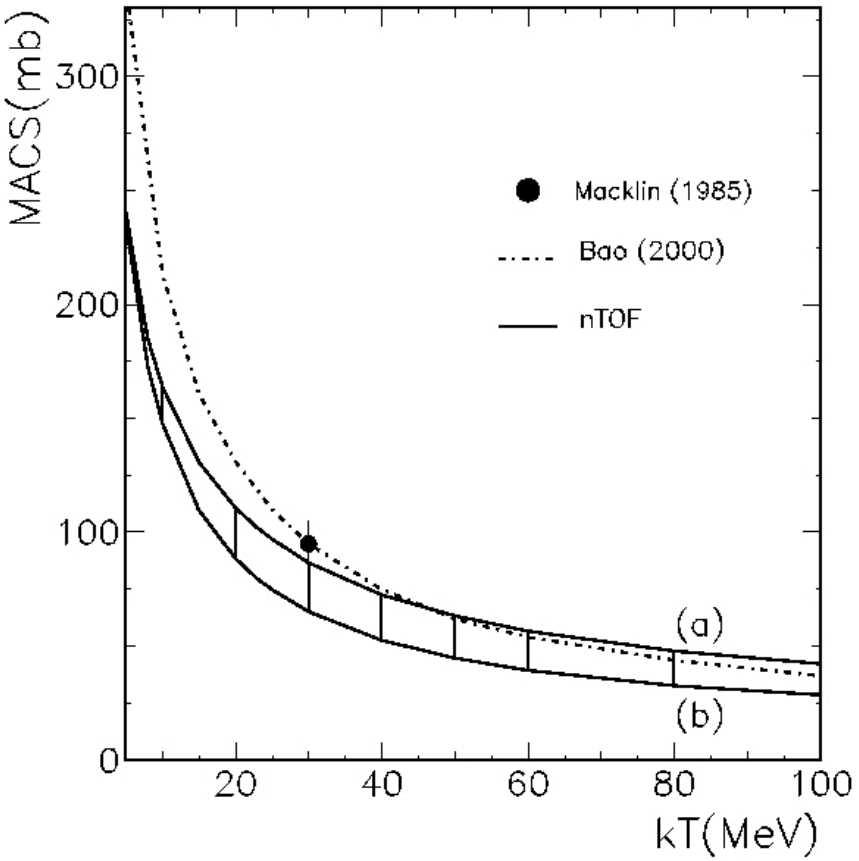

Figure 5: Comparison of present ^{93}Zr MACSs (solid lines), with values from Ref. [13] (dashed line) and the MACS value at 30 keV taken from Ref. [14]. The indices (a) and (b) refer MACS values calculated complementing the n_TOF results with original, evaluated data [12] and by scaling these data by a factor 0.65 (see Fig. 4).

2.1 Implication of the new results.

The results achieved are very important and if confirmed in a wider range of neutron energy could give the solution to persistent questions in the interpretation of the s-process signatures in presolar grains.

Fig. 6 shows the ratio between the elemental Zr and Nb abundances measured in SiC grains (red circles) and predicted by AGB models (calculated for different values of metallicity and stellar mass) [4]. Using the previous capture cross section leads to model predictions (black and open points) in favor of a larger production of Zr with respect of Nb; on the contrary, the n_TOF data (in the more realistic lower limit case for ^{93}Zr) are driving the simulations towards equal contributions of these isotopes, in better agreement with observations. This result is a direct consequence of the new cross section of ^{93}Zr, which results in more ^{93}Zr, and eventually in a higher ^{93}Nb abundance. To settle this issue, it is mandatory to extend the cross section data over a much wider range in neutron energies.

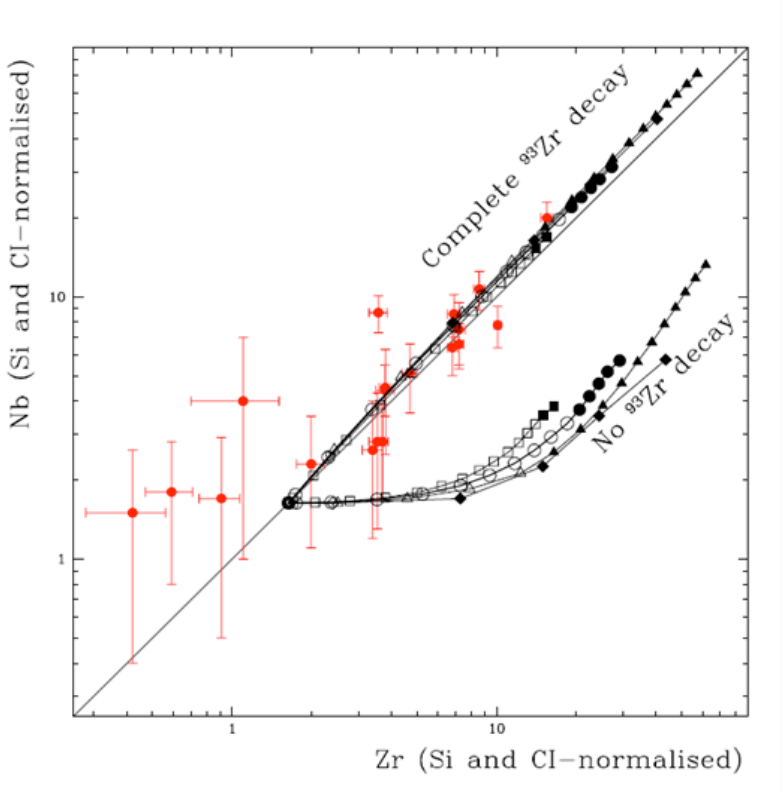

Figure 6 - The Zr and Nb elemental abundances (relative to Si and to CI values of Ref. [4]) measured in single SiC grains and predicted by AGB models. Data are represented by red circles with 2σ standard deviations. Models are represented by black symbols connected by solid lines, where open and full symbols represent third dredge-up episodes resulting in C/O<1 and C/O>1, respectively, at the stellar surface: circle 3 $M_\odot$ Z = 0.02, triangle 3 $M_\odot$ Z = 0.01 squares 3 $M_\odot$ Z = 0.03, diamond 1.8 $M_\odot$ Z = 0.01.

3 New proposed measurement at n_TOF (Phase 2)

Since the n_TOF facility has been upgraded in 2009, the new spallation target is equipped with two different circuits for cooling and moderation, thus offering more flexibility in the choice of the moderator. The use of borated water has reduced the background due to in-beam γ rays by a factor 10 in the energy region above 5 keV as shown in Fig. 7, where the the capture yield of ^{nat}Fe measured with a water moderator is compared with the result obtained with borated water as moderator.

Another improvement of the facility was achieved in 2010, when the experimental area had been upgraded in work sector of class A. This upgrade solves the radioprotection issue due to the radioactivity of the sample, allowing now measurements on unstable samples without a Ti can. For the ^{93}Zr sample this means that the double Al/Ti containment could be substituted by a very muchlighter PEEK ($C_{20}H_{12}O_3$) container as already used in the ^{63}Ni measurement [15]. Fig. 8 illustrates the expected improvement with the new type of canning, which will allow to extend the investigated energy range up to 100 keV. Fig 9 shows a zoom of Fig. 8 in the neutron energy region between 10 – 100 keV.

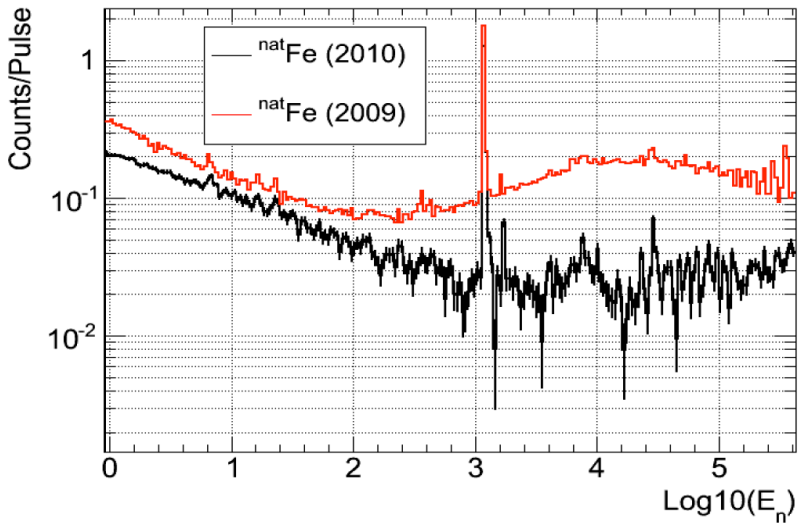

Figure 7: Comparison between the yields of ^{nat}Fe measured in 2009 (red), water was used as moderator, and in 2010 (black), borated water was used as moderator.

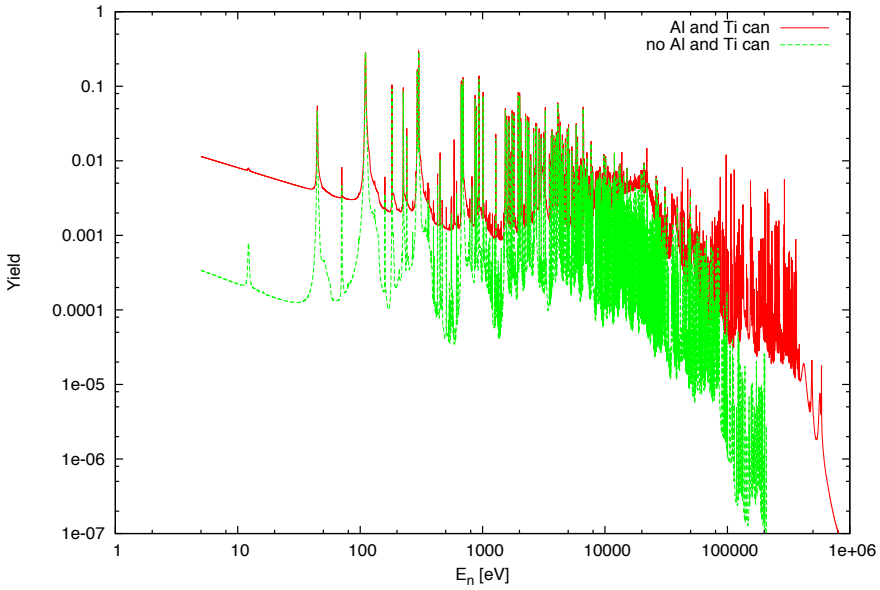

Figure 8 Comparison between the calculated ^{93}Zr yield with (red) and without (green) Al and Ti containers

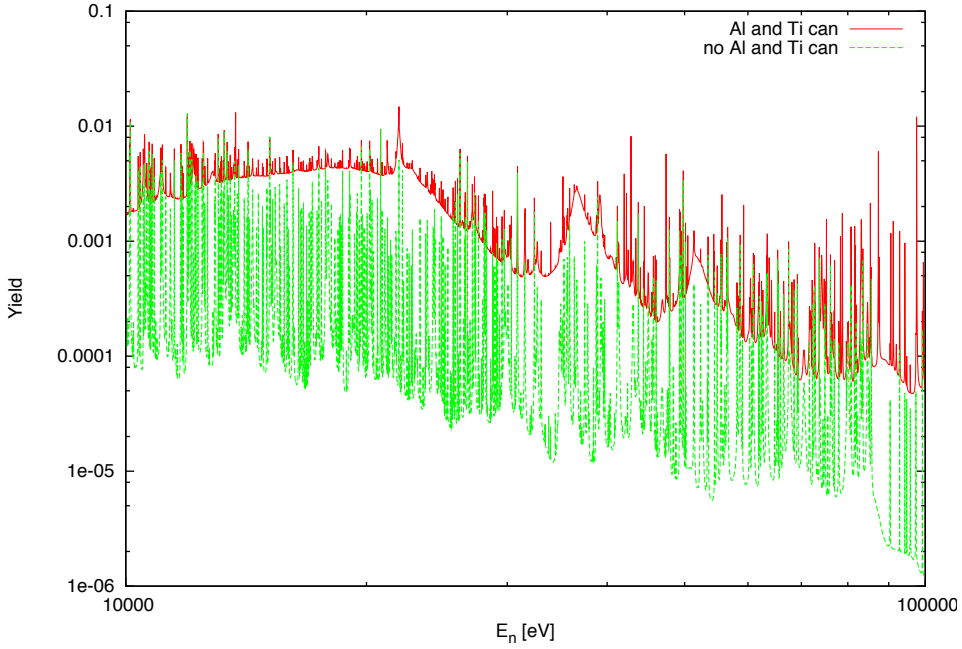

Figure 9 Comparison between the calculated ^{93}Zr yield with and without Al and Ti containers in the neutron energy region between 10 and 100 keV

Summary of requested protons:

We propose to measure the neutron capture cross section of ^{93}Zr taking profit of the upgraded tools available at the n_TOF facility. This cross section will be determined up to 100 keV by means of C_6D_6 liquid scintillators, which are optimized with respect to neutron sensitivity.

The request for the number of protons is based on previous measurements with C_6D_6 scintillation detectors. Together with the ^{93}Zr samples, we plan to measure the yield for ^{92}Zr, Au and C samples as well. ^{92}Zr and Au are used for normalizing the yield and the carbon sample serves for determining the background due to neutrons scattered by the sample.

According to the previous ^{93}Zr measurements we request a total of 3×10^{18} protons for the present measurement.

References:

[1] E.M. Burbidge, G.R. Burbidge, W.A. Fowler, and F. Hoyle, Rev. Mod. Phys., **29** 547 (1957).

[2] R. Gallino, C. Arlandini, M. Busso, M. Lugaro, C. Travaglio, O. Straniero, A. Chieffi, and M. Limongi, Ap. J. **497**, 388 (1998).

[3] C.M. Raiteri, M. Busso, R. Gallino, and G. Picchio, Ap. J. **371**, 665 (1991).

[4] Y. Kashiv et al., Ap. J. **713**, 212 (2010).

[5] Proposal CERN/INTC xxx (2002)

[6] G.Tagliente *et al.* (the n_TOF collaboration), Phys. Rev. C**77**, 035802 (2008)

[7] G.Tagliente *et al.* (the n_TOF collaboration), Phys. Rev. C**78**, 045804 (2008)

[8] G.Tagliente *et al.* (the n_TOF collaboration), Phys. Rev. C**81**, 055801 (2010)

[9] G.Tagliente *et al.* (the n_TOF collaboration), Phys. Rev. C**84**, 015801 (2011)

[10] U. Abbondanno *et al.* the n_TOF collaboration), Nucl. Instr. Meth. **A521** 454 (2004)

[11] S. F. Mughabghab, *Atlas of Neutron Resonances, Resonance Parameters and Thermal Cross Sections Z = 1–100* (Elsevier Science, Amsterdam, 2006).

[12] K. Shibata *et al.*, J. Nucl. Sci. Technol. **48**, 1 (2011); T. Nakagawa, S. Chiba, T. Hayakawa, T. Kajino. Atomic Data Nucl. Data Tables **91** (2005) 77.

[13] Z. Y. Bao, H. Beer, F. K¨appeler, F. Voss, K. Wisshak, and T. Rauscher, At. Data Nucl. Data Tables **76**, 70 (2000).

[14] R.L. Macklin. Astrophysics and Space Science, **115** 71 (1985).

[15] Proposal CERN-INTC 2010-067/INTC-P-283